IOP Publishing Superconductor Science and Technology
Supercond. Sci. Technol. 31 (2018) 065005 (7pp) https://doi.org/10.1088/1361-6668/aabb9b

MgB_2 thick films on three-dimensional structures fabricated by HPCVD

Zhengshan Guo, Xingwei Cai, Xuebin Liao, Yiling Chen, Can Yang, Ruirui Niu, Wenhao Luo, Zigeng Huang, Qingrong Feng and Zizhao Gan

Application Superconductivity Research Center, State Key Laboratory for Artificial Microstructure and Mesoscopic Physics, School of Physics, Peking University, Beijing 100871, People's Republic of China

E-mail: xwcai@pku.edu.cn

Received 16 January 2018, revised 27 March 2018
Accepted for publication 4 April 2018
Published 30 April 2018

Abstract

Magnetic shielding has been a key factor in the measurement of ultra-weak magnetic fields, especially for shielding from low frequency electromagnetic noise. With the recent development of superconducting quantum interference devices, superconducting magnetic shielding has become an important area of research. MgB_2 has shown great potential in magnetic shielding for its remarkable superconducting properties, the feasibility of its use in this capacity having been demonstrated by MgB_2 bulk samples. However, the potential for application of such bulk samples is limited. In this work, we have investigated the possibility of the fabrication of MgB_2 films on three-dimensional (3D) structures using a hybrid physical−chemical vapor deposition system. MgB_2 films 10 μm thick have been fabricated on the outer surface of a polycrystalline Al_2O_3 cylinder. The deposited film showed a transition temperature (T_C) of 39 K and J_C of 5.1×10^5 A · cm^{-2}, which are comparable to those of planar MgB_2 films. This work shows the feasibility of depositing MgB_2 films onto a 3D structure, and sheds light on the potential use of MgB_2 films in superconducting magnetic shielding.

Keywords: magnesium diboride, thick film deposition, HPCVD

(Some figures may appear in colour only in the online journal)

1. Introduction

The binary intermetallic compound MgB_2 has attracted great interest in both fundamental studies and practical applications since its superconductivity was discovered in 2001 [1]. Due to its remarkable superconducting properties, such as high superconducting transition temperature (T_C) of 39 K [2], simple crystalline structure, high critical current density (J_C) [3], and absence of weak links at grain boundaries [4], MgB_2 is considered to be one of the most promising superconducting materials for such applications as medium-strength superconducting magnets [5], Josephson junction devices [6], and digital circuits [7]. Various forms of MgB_2, such as films, tapes, polycrystalline wires, micro whiskers, etc, have been fabricated in the past few decades [8–12]. Among these, MgB_2 films are highly valued because of their outstanding performance and flexibility in practical application.

A variety of methods have been developed to fabricate MgB_2 films, including pulsed laser deposition [13], molecular beam epitaxy (MBE) [14], electron beam evaporation [15], and hybrid physical−chemical vapor deposition (HPCVD) [3]. Among these techniques, HPCVD seems to be the most effective way to fabricate high-performance MgB_2 films from several nanometers to dozens of micrometers thick [3, 16–20]. Most of the research on HPCVD has focused on planar surfaces, as planar MgB_2 films can be used in many applications like kinetic inductance detectors [21], superconducting quantum interference devices (SQUIDs) [5], and hot-electron bolometer mixers [22], etc. However, in some cases, non-planar MgB_2 films are needed—such as superconducting radio frequency (SRF) cavities [23, 24], magnetic shielding tubes [5], etc, where MgB_2 films are required to be fabricated on three-dimensional (3D) structures. In our previous work, the experiment of fabricating MgB_2 planar films on stainless steel and then bending it to a certain angle has been conducted. Cracks between films and substrate arose

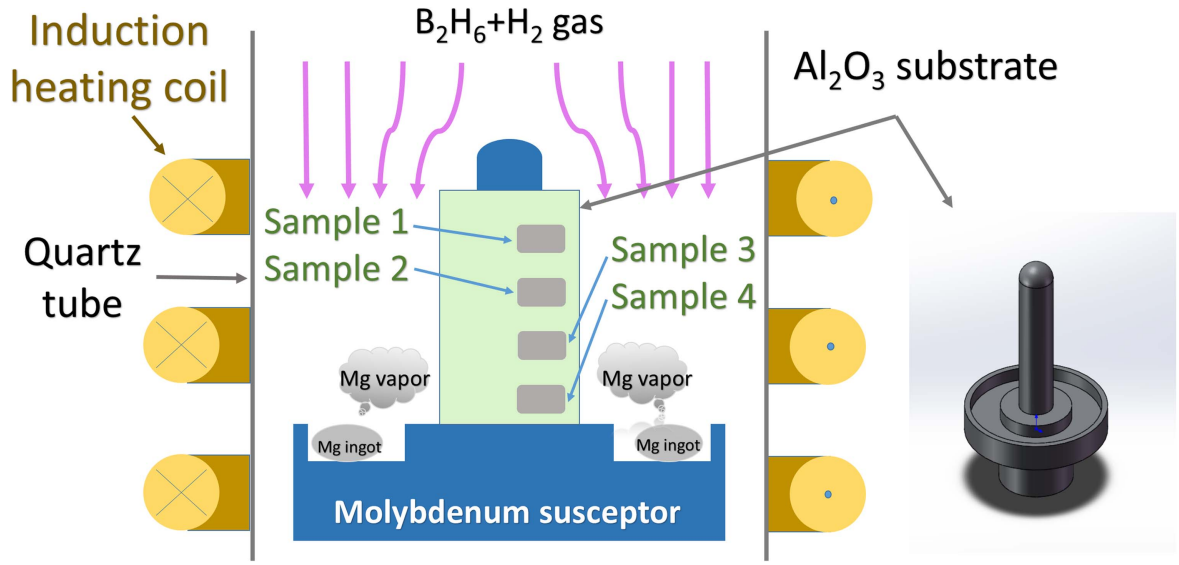

Figure 1. Schematic of the modified HPCVD system. The image to the right is a 3D depiction of the molybdenum susceptor. The hollow Al_2O_3 cylindrical substrate is set on a molybdenum cylinder.

with increasing bend angle, which degraded the performance of superconducting films [25]. Therefore, the study of techniques to fabricate such films on three-dimensional structures is needed.

Anti-electromagnetic interference plays an important role in the measurement of ultra-weak magnetic signals, especially for low frequency interference. For example, the most sensitive magnetic detector SQUID usually needs to be put in a magnetic shielding tube to obtain high resolution for magnetic fields. Superconducting magnetic shielding (SMS) has an outstanding shielding effect against both high and low frequency interference. Low temperature SMS has been successfully developed using niobium, and Nd_3Sn and has been widely used, while SMS above liquid helium temperature is still unavailable. As a medium temperature superconducting material, MgB_2 is a material of interest for high temperature SMS [26]. The magnetic shielding capability of MgB_2 has previously been verified using MgB_2 bulk cylinders [5, 27, 28], but the dimensions and geometric shapes of magnetic shielding tubes for which this form can be used are limited. Three-dimensional MgB_2 films can maintain the magnetic shielding capability while meeting the dimension and outline demands of a range of technical needs, whence they have great research value. Very recently, Xi *et al* tried to fabricate MgB_2 films directly inside a Cu tube to meet the demand of SRF cavities, and got promising results [29, 30]; the T_C is in the range of 30–38 K, which indicates that HPCVD can be used in 3D film fabrication. For magnetic shielding, non-metal tubes with thick MgB_2 films are required. Films fabricated on non-metal 3D structure need to be studied.

In this work, we report the fabrication of MgB_2 thick films on a cylindrical structure of polycrystalline Al_2O_3 by HPCVD. High-performance MgB_2 films of 10 μm thickness were obtained. The T_C values of the films were above 39 K, comparable with those of planar films fabricated by HPCVD. Microstructure and conducting performance of the film have been studied.

2. Experiments

The detailed setup of HPCVD has been described in previous articles [31]. A modified HPCVD system was built to fabricate MgB_2 thick films on the outside surfaces of 3D structures. The schematic diagram of the HPCVD system is shown in figure 1. The growth of MgB_2 films during HPCVD is sensitive to the annealing temperature. To make sure the outer surface of the 3D structure had a uniform temperature distribution, an induction heating apparatus was used as the heating source, replacing the conventional resistive coil. A quartz tube instead of a stainless steel cylinder was assembled as a reactor chamber so that induction heating on the sample could be easily controlled. In this work, thick MgB_2 films were deposited on the outer surfaces of polycrystalline Al_2O_3 hollow cylinders (the outside diameter being 18 mm and inner diameter 12 mm). A specially designed molybdenum susceptor (figure 1) was used as a sample holder and inductive heating source. The Al_2O_3 hollow cylindrical substrate was set on the molybdenum cylinder. Mg ingots (99.5% in purity) with masses of 3–4 g were placed on the susceptor as the Mg source. A gas mixture of 25% diborane (B_2H_6) and 75% hydrogen was used as the boron source.

During MgB_2 film growth, ultra-high purity hydrogen gas (99.9999%) was introduced into the chamber as ambient gas at a flow rate of 300 sccm and a pressure of 5 kPa, to provide a reducing reaction environment. Next, the substrate and solid Mg ingots along with the susceptor were heated up inductively to the set temperature of 610 °C. When the Mg ingots started to melt at ~550 °C, mixed B_2H_6 gas was introduced at the flow rate of 10 sccm into the reactor. The temperature was then fixed at 610 °C for 15 min with the

Table 1. Positions (distinguished by vertical distance from the susceptor) and thickness of the samples.

	Sample 1	Sample 2	Sample 3	Sample 4
Position (mm)	2.5	7.5	12.5	17.5
Thickness (μm)	8.9	9.9	11.2	

pressure stabilized at around 6 kPa. B_2H_6 met the Mg vapor at the induction heating region and reacted to form MgB_2 which was deposited on the surface of the cylindrical substrate. Finally, the fabricated films were cooled down to room temperature in flowing H_2 gas.

The thickness of each sample was measured using a stylus profiler (AlphaStep D-500) after chemically etching a step on the films. The phase purity and crystallinity were analyzed using a Philp X'pert x-ray diffractometer (XRD). The surface micromorphology of the MgB_2 films were characterized using a scanning electron microscope (FEI NOVA Nano-SEM 430). The temperature-dependent resistance (ρ-T curve) was carried out using the standard four-probe method. The critical current densities J_C were calculated using the Bean model from the magnetization hysteresis loops (M-H curve) obtained from a Quantum Design Magnetic Property Measurement System (MPMS-7).

3. Results and discussion

To study the variation of the superconducting property of the film with changes in position, four small sample pieces were cut out from different regions (figure 1) and distinguished by the vertical distance from the susceptor, as shown in table 1. Note that thicker films were deposited on the lower samples, where higher Mg vapor pressure can be expected. The average thicknesses measured were as shown in table 1 except for Sample 4, the thickness of which could not be measured specifically. Dendritic Mg deposition was found on top of Sample 4, which created large errors in thickness measurements. As for the other samples, the thickness increased slightly as the distance from the bottom of the susceptor decreased. From samples 2 and 3, at the optimum deposition position, an average thickness of 10 μm was measured. A deposition rate of 11.1 nm s^{-1} can be calculated, which is higher than that of conventional HPCVD [3, 16–18]. The deposition rate is determined by the pressure of Mg vapor and the flow rate of B_2H_6. The variation of the thickness of the film at the same height is less than 1 μm.

The crystalline structure of the films was explored by XRD, and is shown in figure 2. From Sample 1 to Sample 3, the intensity of Al_2O_3 peak gradually decreased while the intensity of MgB_2 peaks increased, which indicates that the MgB_2 film had a polycrystalline structure and became denser and thicker as it was placed lower and closer to the Mg source. Impurities of Mg and MgO can also be noticed in the MgB_2 films, which were mainly caused by the re-deposition of residual Mg vapor during the cooling process. This is most significant in the XRD pattern of sample 4, which was close

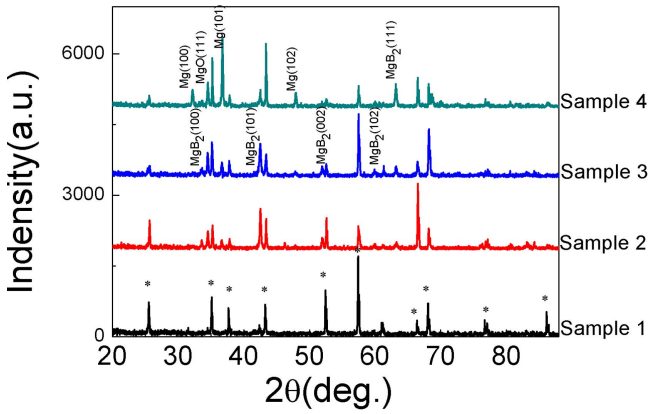

Figure 2. XRD patterns of the samples. Peaks corresponding to the Al_2O_3 substrate are shown in this figure marked by '*'.

to the Mg source. It can be seen that the Mg peaks increased, while most of the MgB_2 peaks dropped. The SEM images of the samples reconfirmed this conclusion. As a result, Mg vapor pressure is seen to play a very important role in the difference between the samples; maintaining a uniform Mg vapor pressure inside the chamber is crucial in this work. In the upper region (Sample 1), where Mg vapor is insufficient, decomposition of B_2H_6 happened as $B_2H_4 \rightarrow B\downarrow + H_2$; boron was deposited on the substrate directly, instead of MgB_2. As the Mg vapor pressure increased in the lower region, MgB_2 formation dominated the deposition process. But when the Mg vapor pressure was too high (as in Sample 4), re-deposition of the saturated Mg vapor occurred on the substrate surface, contaminating the MgB_2 film; in our system, controlling Mg vapor pressure proved to be the difficult part. The evaporation rate of Mg is affected by the deposition of MgB_2 on the surface of Mg ingots.

The SEM images of the MgB_2 thick films are shown in figure 3. All the samples had polycrystalline structures. It can be observed from figures 3(a)–(d) that the substrates were completely coated with dense films, while granular structures of $\sim$10 μm were found on top of the film. Beneath the granular structures, the films of sample 2 and 3 are more dense and solid than sample 1 as more Mg vapor was available at lower positions. The dense films under the clusters demonstrated relatively good conductivity. In the image of Sample 4, a lot of brightly-colored Mg clusters were discovered. As it was placed near the Mg source, a lot of Mg redeposition happened. These granules inevitably affected the T_C measurement, with lower T_C and nonzero resistance transition. Figures 3(e) and (f) showed magnified view of the top isolated clusters and the bottom of sample 3 respectively. It can be observed that both them are composed by hexagonal crystallites of about 1–2 μm in size. The MgB_2 grains in figure 3(e) present as good hexagonal prisms, fitting its hexagonal crystal structure, with the (0001) and (1100) planes being the faces with slower growth rate. As the deposition was conducted on polycrystalline Al_2O_3 substrate, no textured epitaxial growth was found. The Volmer−Weber mode growth [2, 32] of the MgB_2 hexagonal prisms resulted in some voids and gaps between the grains. In the isolated

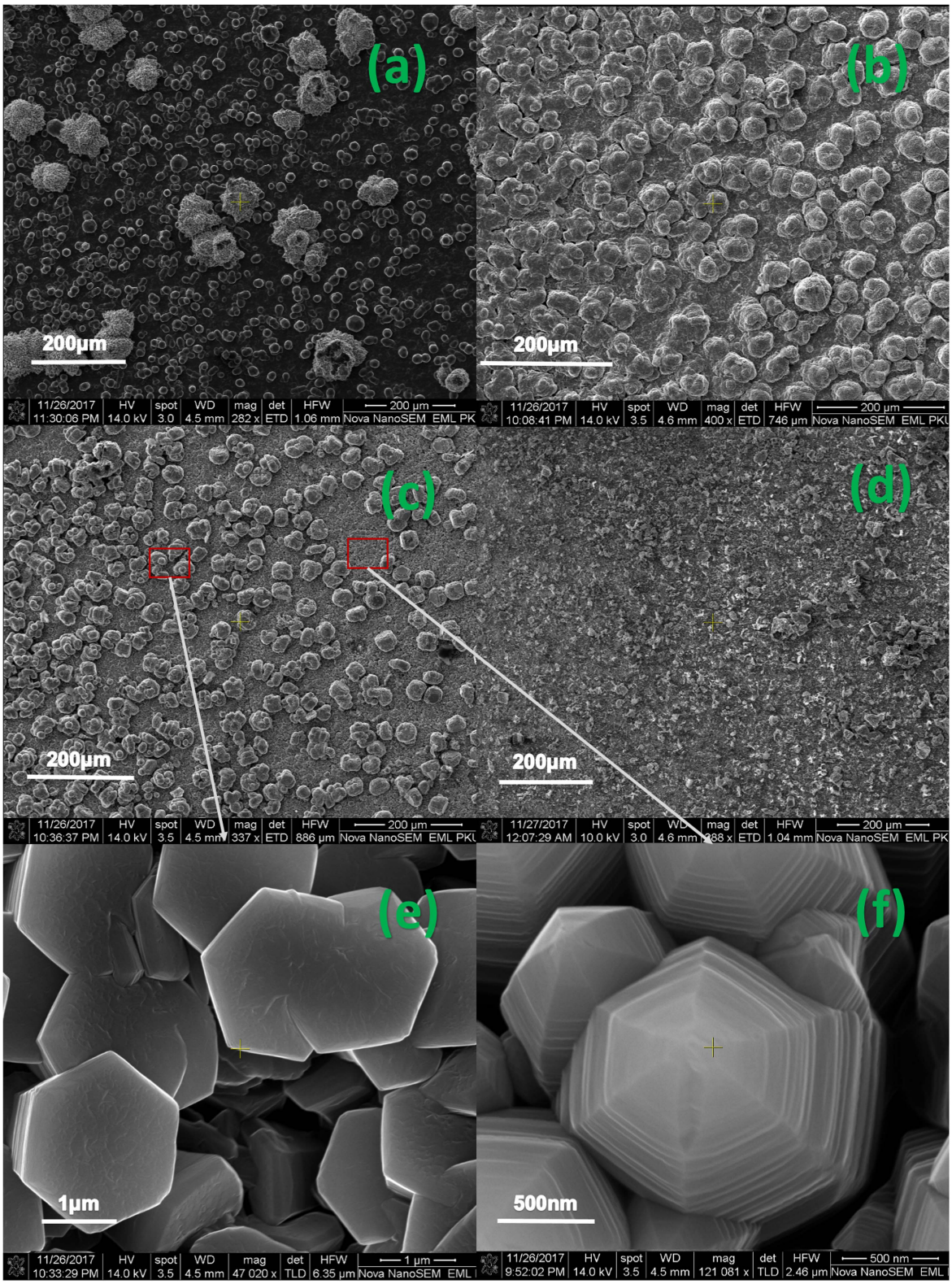

Figure 3. (a)–(d) SEM images of the four samples. (e)–(f) Magnified view of the top isolated granule and the bottom microcrystal grain of sample 3.

clusters (figure 3(f)), step-pyramid shaped grains were observed. This might indicate that the Mg vapor was depleted on the substrate surface, so that the crystal growth tended to reach out for more Mg vapor. Similarly pyramid shaped MgB_2 grains have been observed on Al_2O_3 substrate by Won *et al* [33]. Above all, controlling the Mg vapor pressure is the crucial controlling factor.

Figure 4 shows the temperature dependence of the resistivity of the various samples. It can be observed that all four samples exhibited a superconducting transition, while T_C

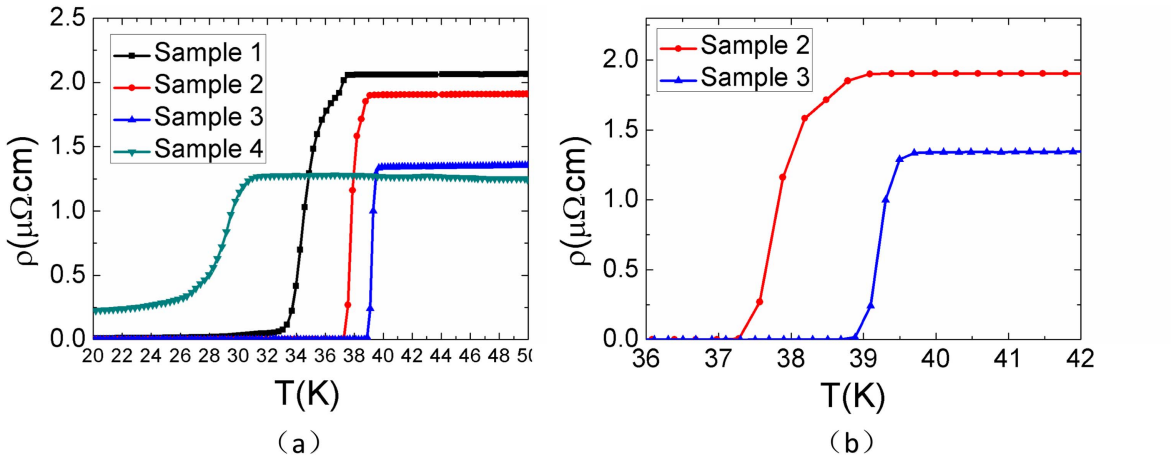

Figure 4. (a) Temperature dependence of the resistivity of the various samples. (b) Magnified view around the superconducting transition region of Samples 2 and 3.

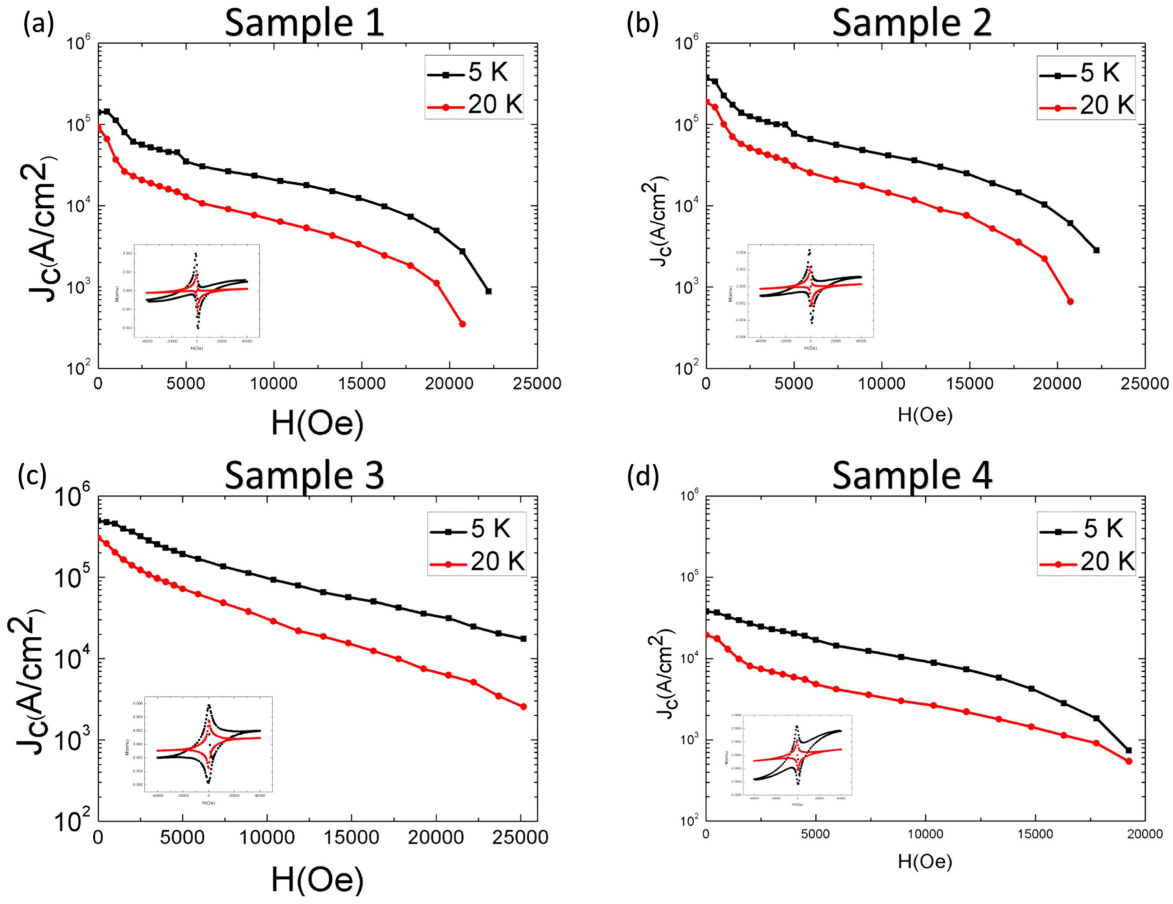

Figure 5. Magnetic field dependence of J_C of the various samples. Insets display the respective magnetic hysteresis loops measured at 5 and 20 K.

varied with the change of position. Samples 2 and 3 respectively had onset transition temperatures of 38.9 K and 39.6 K with sharp transition widths of about 0.8 K and 0.6 K, comparable with those of high-quality planar MgB_2 films fabricated on single crystal substrates by HPCVD. However, the T_C of Samples 1 and 4 was lower. Due to the insufficiency of Mg vapor, the T_C of Sample 1 decreased to 36.8 K, and the corresponding transition width increased to 2.5 K. Meanwhile, Sample 4 displayed a performance reduction of the T_C to 30.3 K and ΔT_C to 4.2 K, and a high residual resistance was measured when the superconducting transition completed. As the position was close to the Mg source, the Mg vapor around Sample 4 was the highest among four positions and a lot of Mg granules re-deposited and contaminated the film—which was also observed using the SEM. The Mg granules may cause a short-circuit between the

current and voltage probes in the four-probe method, leading to voltage pick-up. The ρ-T results indicate that we can develop high T_C MgB_2 films on 3D structures by HPCVD with induction heating. The area of high-quality films is sensitive to the position in vertical direction between the Mg source and the B_2H_6 gas. It is also influenced by the position in the induction coil, which determines the heating/temperature distribution.

The magnetic field dependence of J_C was calculated from the magnetization hysteresis loops using the Bean model [34] $J_C = 20\Delta M/[Va(1 - a/3b)]$, where ΔM is the height difference of the M-H loop, V is the volume of film, and a, b are the sample dimensions with $a < b$. The J_C-H curves are shown in figure 5. The J_C (0) at 5 K for samples 1 to 4 were 1.4×10^5, 3.8×10^5, 5.1×10^5, and 3.8×10^4 A · cm^{-2} respectively. These J_C values are lower than those on single crystal Al_2O_3 or SiC substrate [17]. As is shown in figure 3, the films we obtained have a lot of voids and gaps inside, which potentially affect the current carrying capacity of the films and lead to a decrease of J_c. However, the J_C (0) values of samples 2 and 3 are close to that of MgB_2 planar films fabricated on metal substrates [18, 23]. The J_C result is predictable, as the substrates we used are polycrystalline, the growth mode thus being non-epitaxial and leading to inevitable voids in the films. On the other hand, the fast deposition rate further increased the number of those voids. The comparison of the four J_C-H curves also shows that Samples 2 and 3 have better superconducting performance than Samples 1 and 4, which indicates that with specifically controlled growth conditions, an increase in J_C could be expected. The low value J_C for Sample 4 might be caused by the poor connection between grains in the film, which is a result of Mg contamination. In the M-H diagram (inserts in figure 5), distortion of the M-H loop has been overserved. The distortion of the loops is related to the flux pinning in the non-epitaxial MgB_2 films. Similar distortion can be observed in YBCO research [35, 36].

4. Conclusion

In this work, we studied the fabrication of MgB_2 thick films by HPCVD on non-metal 3D structures, which is needed in magnetic shielding. The films were fabricated on polycrystalline Al_2O_3 cylinders, and showed a high transition temperature of 39 K; a high deposition rate was obtained, proving the feasibility of the method. The critical current density was $\sim 10^5$ A · cm^{-2}, lower than that of planar MgB_2 films on single crystal substrate, but comparable with results on metal substrate. The lowering of J_C is possibly due to voids and discontinuities caused by the non-epitaxial Volmer −Weber mode growth of MgB_2 and fast deposition rate. The size of MgB_2 films produced is of the order of centimeters, which is suitable for SQUID or other high resolution magnetic detectors and meets the demand of superconducting magnetic shielding. This is the first time that HPCVD MgB_2 films have been fabricated on 3D ceramic structures for magnetic shielding. In future experiments, the shielding effect will be tested, and further optimization of the system done to deposit higher quality MgB_2 films on larger 3D structures. A MgB_2 film superconducting magnetic shielding device for magnetic detectors working at a temperature of 20–40 K will be built.

Acknowledgments

This work was supported by the National Basic Research Program of China (Grant 2011CBA00104).

ORCID iDs

Xingwei Cai https://orcid.org/0000-0003-2008-0661

References

[1] Nanamatsu J, Norimasa N, Muranaka T, Zenitani Y and Akimitsu J 2001 Superconductivity at 39 K in magnesium diboride *Nature* **410** 63–4
[2] Xi X X *et al* 2007 MgB_2 thin films by hybrid physical–chemical vapor deposition *Physica* C **456** 22–37
[3] Zhuang C G, Meng S, Zhang C Y, Feng Q R, Gan Z Z, Yang H, Jia Y, Wen H H and Xi X X 2008 Ultrahigh current-carrying capability in clean MgB_2 films *J. Appl. Phys.* **104** 013924
[4] Canfield P C, Bud'Ko S L and Finnemore D K 2002 An overview of the basic physical properties of MgB_2 *Physica* C **85** 1–7
[5] Rabbers J J, Oomen M P, Bassani E, Ripamonti G and Giunchi G 2010 Magnetic shielding capability of MgB 2 cylinders *Supercond. Sci. Technol.* **23** 125003
[6] Hu H, Feng Q, Wang Y and Zhang Y 2015 The study of MgB_2/BN/MgB_2 trilayer films *Physica* C **519** 85–8
[7] Zeng X H *et al* 2002 *In situ* epitaxial MgB_2 thin films for superconducting electronics *Nat. Mater.* 31–8
[8] Kang W N, Kim H J, Choi E M, Jung C U and Lee S I 2001 MgB_2 superconducting thin films with a transition temperature of 39 kelvin *Science* **292** 1521–3
[9] Kumakura H, Matsumoto A, Fujii H and Togano K 2001 High transport critical current density obtained for powder-in-tube-processed MgB_2 tapes and wires using stainless steel and Cu–Ni tubes *Appl. Phys. Lett.* **79** 2435–7
[10] Wu Y, Messer B and Yang P 2001 Superconducting MgB_2 nanowires *Adv. Mater.* **13** 1487–9
[11] Nath M and Parkinson B A 2007 Superconducting MgB_2 nanohelices grown on various substrates *J. Am. Chem. Soc.* **129** 11302–3
[12] Wang Y, Zhuang C, Gao J, Shan X, Zhang J, Liao Z, Xu H, Yu D and Feng Q 2009 MgB_2 superconducting whiskers synthesized by using the hybrid physical−chemical vapor deposition *J. Am. Chem. Soc.* **131** 2436–7
[13] Wu Y S, Zhao Y, Wexler D, Kim J H and Dou S X 2008 Optimization of *in situ* annealing conditions for off-axis PLD MgB_2 films *Physica* C **468** 218–22
[14] Takahashi T, Harada Y, Iriuda H, Kuroha M, Oba T, Seki M, Nakanishi Y, Echigoya J and Yoshizawa M 2006 Transmission electron microscopy study of as-grown MgB_2 films *Physica* C **445–448** 887–90
[15] Zhu H M, Zhang Y B, Sun X L, Xiong W J and Zhou S P 2007 MgB_2 thin films on Si(111) without a buffer layer prepared by e-beam evaporation *Physica* C **452** 11–15

[16] Yuhao Z, Zhiyuan L, Qian D, Dongyao L, Yinbo W, Yan Z, Yue W and Qingrong F 2011 Ultrathin MgB_2 films fabricated on Al_2O_3 substrate by hybrid physical–chemical vapor deposition with high T_c and J_c *Supercond. Sci. Technol.* **24** 015013

[17] Chen Y, Yang C, Jia C, Feng Q and Gan Z 2016 Thickness dependence of $J_c(0)$ in MgB_2 films *Physica* C **525–526** 56–60

[18] Fa H, Da-tao X, Qing-rong F and Ke-xin L 2012 MgB 2 films fabricated on molybdenum substrate by hybrid physical–chemical vapor deposition for superconducting RF cavity applications *Supercond. Sci. Technol.* **25** 065003

[19] Seong W K and Kang W N 2008 Superconductivity of epitaxial MgB_2 thick films and MgB_2 nanowires grown by hybrid physical–chemical vapor deposition *Physica* C **468** 1884–7

[20] Chen Y, Liao X, Cai X, Yang C, Guo Z, Niu R, Zhang Y, Jia C and Feng Q 2017 Superconducting joint for MgB2 thin films by sol-gel method *Physica* C **542** 34–9

[21] Yang C, Niu R R, Guo Z S, Cai X W, Chu H M, Yang K, Wang Y, Feng Q R and Gan Z Z 2018 Lumped element kinetic inductance detectors based on two-gap MgB_2 thin films *Appl. Phys. Lett.* **112** 022601

[22] Xu Z, Kong X, Han L, Pang H, Wu Y, Gao Z and Li X 2017 Elimination of bubbles and improvement of the superconducting properties in MgB_2 films annealed using electron beam *Supercond. Sci. Technol.* **30** 035013

[23] Zhimao N, Xin G, Paul B W, Can Y, Matthew F, Sami T, Qingrong F and Kexin L 2017 Fabrication and radio frequency test of large-area MgB_2 films on niobium substrates *Supercond. Sci. Technol.* **30** 045009

[24] Guo X, Ni Z, Chen L, Hu H, Yang C, Feng Q and Liu K 2016 Using helium as background gas to avoid hydrogen brittleness for MgB_2 film fabrication on niobium substrate by HPCVD *Physica* C **524** 13–7

[25] Wang Y B, Chen Y L and Feng Q R 2012‘ The effect of nano-particles in superconducting MgB_2 thin films on stainless steel substrates *Smart Technologies for Materials, Advanced Materials Research* ed T H Chang pp 62–7(Zurich: Trans Tech)

[26] Clem T 1985 Superconducting magnetic shielding for SQUID-based systems operating in low fields *IEEE Trans. Magn.* **21** 606–9

[27] Gozzelino L, Minetti B, Gerbaldo R, Ghigo G, Laviano F, Agostino A and Mezzetti E 2011 Local magnetic investigations of MgB_2 bulk samples for magnetic shielding applications *IEEE Trans. Appl. Supercond.* **21** 3146–9

[28] Giunchi G, Turrioni D, Kashikhin V, Nguyen H and Barzi E 2016 Feasibility study of a MgB_2 superconducting magnetic cloak *IEEE Trans. Appl. Supercond.* **26** 8801005

[29] Lee N, Withanage W K, Tan T, Wolak M A, Nassiri A and Xi X 2017 Hybrid physical chemical vapor deposition of magnesium diboride inside 3.9 GHz mock cavities *IEEE Trans. Appl. Supercond.* **27** 3500304

[30] Withanage W K, Lee N, Penmatsa S V, Wolak M, Nassiri A and Xi X 2017 Magnesium diboride on inner wall of copper tube: a test case for superconducting radio frequency cavities *Phys. Rev. Accel. Beams* **20** 102002

[31] Xi X X 2009 MgB 2 thin films *Supercond. Sci. Technol.* **22** 043001

[32] Chenggang Z, Ke C, Joan M R, Qi L and Xi X X 2010 Surface morphology and thickness dependence of the properties of MgB_2 thin films by hybrid physical–chemical vapor deposition *Supercond. Sci. Technol.* **23** 055004

[33] Seong W K, Ranot M, Lee J Y, Yang C W, Lee J H, Oh Y H, Ahn J P and Kang W N 2016 Superconducting MgB_2 flowers: growth mechanism and their superconducting properties *Supercond. Sci. Technol* **29** 045015

[34] Bean C P 1962 Magnetization of hard superconductors *Phys. Rev. Lett.* **8** 250

[35] Yoo S I, Sakai N, Higuchi T and Murakami M 1995 Melt processing for obtaining $REBa_2/Cu_3/O_y$ superconductors (RE = Nd, Sm) with high T_c and large J_c *IEEE Trans. Appl. Supercond.* **5** 1568–71

[36] Yoo S I, Sakai N, Kojo H, Takebayashi S, Hayashi N, Takahashi M, Sawada K, Higuchi T and Murakami M 1997 Progress in melt processing of Nd-Ba-Cu-O superconductors *IEEE Trans. Appl. Supercond.* **7** 1781–6